

POWER ASYMMETRY IN WMAP AND PLANCK TEMPERATURE SKY MAPS AS MEASURED BY A LOCAL VARIANCE ESTIMATOR

Y. AKRAMI¹, Y. FANTAYE^{1,2}, A. SHAFIELOO^{3,4}, H. K. ERIKSEN¹, F. K. HANSEN¹, A. J. BANDAY^{5,6}, K. M. GÓRSKI^{7,8}

Draft version December 3, 2024

ABSTRACT

We revisit the question of hemispherical power asymmetry in the WMAP and Planck temperature sky maps by measuring the local variance over the sky and disks of various sizes. For the 2013 Planck sky map we find that none of the 1000 available isotropic Planck “Full Focal Plane” (FFP6) simulations have a larger variance asymmetry than that estimated from the data, suggesting the presence of an anisotropic signature formally significant at least at the 3.3σ level. For the WMAP 9-year data we find that 5 out of 1000 simulations have a larger asymmetry. The preferred direction for the asymmetry from the Planck data is $(l, b) = (212^\circ, -13^\circ)$, in good agreement with previous reports of the same hemispherical power asymmetry.

Subject headings: cosmic microwave background — cosmology: observations — methods: statistical

1. INTRODUCTION

The assumptions of statistical isotropy and homogeneity of the Universe on very large scales, jointly called the cosmological principles, are two of the main pillars of our present standard model of cosmology. In the past, the validity of these assumptions was based largely on philosophical arguments, or as a necessity in order to simplify otherwise complicated equations. Today, the situation is very different. With the advent of advanced space and ground-based instruments, stringent tests of these basic assumptions are available.

Indeed, almost immediately after the first release of the measurements of the cosmic microwave background (CMB) temperature fluctuations by the Wilkinson Microwave Anisotropy Probe (WMAP) experiment (Bennett *et al.* 2003), different groups found various anomalous features in the data that hinted at possible violations of the statistical isotropy (see e.g. Tegmark *et al.* 2003; de Oliveira-Costa *et al.* 2004; Vielva *et al.* 2004; Larson and Wandelt 2004; Land and Magueijo 2005a,b; McEwen *et al.* 2005, 2006; Jaffe *et al.* 2006; Hinshaw *et al.* 2007; Spergel *et al.* 2007; Cruz *et al.* 2007; Bridges *et al.* 2007; Copi *et al.* 2007; Land and Magueijo 2007; Bernui *et al.* 2007; Bernui and Hipolito-Ricaldi 2008; Pietrobon *et al.* 2008). Among these was one suggesting a directional

dependency of the CMB angular power spectrum (Eriksen *et al.* 2004; Hansen *et al.* 2004), often referred to as a “hemispherical power asymmetry”. Since then, this observation has been probed with different methods and algorithms, and is with current data sets generally found to be statistically significant at the $3 - 3.5\sigma$ level depending on the algorithm and angular scales under considerations (Park 2004; Eriksen *et al.* 2007; Hansen *et al.* 2009; Hoftuft *et al.* 2009; Axelsson *et al.* 2013; Ade *et al.* 2013a). Accordingly, theorists are now attempting to reconcile these observations with the current cosmological standard model (see e.g. Erickcek *et al.* 2008; Dai *et al.* 2013; Lyth 2013; Liddle and Corts 2013; Mazumdar and Wang 2013; Namjoo *et al.* 2013; Abolhasani *et al.* 2013; Cai *et al.* 2013; Kohri *et al.* 2013; McDonald 2013; Kanno *et al.* 2013).

Gordon *et al.* (2005) suggested that the power asymmetry might be modelled in terms of a dipole modulation of the form

$$\frac{\Delta T}{T} |_{\text{mod}}(\hat{n}) = (1 + A \hat{n} \cdot \hat{p}) \frac{\Delta T}{T} |_{\text{iso}}(\hat{n}), \quad (1)$$

where $\frac{\Delta T}{T} |_{\text{iso}}$ and $\frac{\Delta T}{T} |_{\text{mod}}$ are, respectively, the isotropic and modulated CMB temperature fluctuations along a direction \hat{n} on the sky, A is the amplitude of the dipole modulation and \hat{p} is the preferred direction. Direct likelihood fits of this particular model have been reported by Eriksen *et al.* (2007); Hoftuft *et al.* (2009); Ade *et al.* (2013a) for the WMAP and Planck (Ade *et al.* 2013b) data, obtaining a typical dipole modulation amplitude of $A \sim 0.07$ on large angular scales, statistically significant at $\sim 3\sigma$. Equivalent results have been obtained using for instance the BiPolar Spherical Harmonics (BiPoSHs) technique (Hajian and Souradeep 2003, 2006; Ade *et al.* 2013a). On small angular scales, the dipole amplitude is much lower, and appears to vanish by a multipole moment of $\ell \sim 500-600$ (Hansen *et al.* 2009; Ade *et al.* 2013a).

However, there is a significant debate in the field concerning whether these findings are statistically significant

yashar.akrami@astro.uio.no
y.t.fantaye@astro.uio.no
arman@apctp.org

¹ Institute of Theoretical Astrophysics, University of Oslo, P.O. Box 1029 Blindern, N-0315 Oslo, Norway

² Department of Mathematics, University of Rome Tor Vergata, Rome, Italy

³ Asia Pacific Center for Theoretical Physics, Pohang, Gyeongbuk 790-784, Korea

⁴ Department of Physics, POSTECH, Pohang, Gyeongbuk 790-784, Korea

⁵ Université de Toulouse, UPS-OMP, IRAP, F-31028 Toulouse cedex 4, France

⁶ CNRS, IRAP, 9 Av. colonel Roche, BP 44346, F-31028 Toulouse cedex 4, France

⁷ Jet Propulsion Laboratory, California Institute of Technology, 4800 Oak Grove Drive, Pasadena, California, U.S.A.

⁸ Warsaw University Observatory, Aleje Ujazdowskie 4, 00-478 Warszawa, Poland

after accounting for so-called “look-elsewhere” effects,⁹ or if they could simply be the product of so-called *a-posteriori* statistical inference¹⁰ (see e.g. [Bennett et al. 2011](#)). Demonstrating robustness with respect to statistics and data selection can to some extent alleviate such criticisms. With this in mind, we study in this paper the question of statistical isotropy from the simplest possible point of view, namely by computing the local variance of the CMB fluctuations over patches of different sizes and positions on the sky, and comparing these measurements with those obtained from isotropic simulations. Related variance-oriented studies have been performed for example by [Bernui et al. \(2007\)](#); [Bernui and Hipolito-Ricardi \(2008\)](#); [Lew \(2008a,b\)](#); [Rath and Jain \(2013\)](#).

2. DATA AND METHOD

We include in the following analysis the foreground-reduced co-added V (61 GHz) and W (94 GHz) temperature sky maps from the 9-year WMAP data release, and the SMICA map from the Planck 2013 data release ([Ade et al. 2013c](#)); the three other Planck CMB temperature solutions (Commander–Ruler, NILC and SEVEM) give consistent results, and are omitted in the following for brevity. To exclude pixels that are highly contaminated by diffuse foreground emission and point sources, we adopt the WMAP9 KQ85 Galactic and point source mask, with a sky coverage of $\sim 75\%$, for the WMAP data, and the Planck standardized common mask, U73, with a sky coverage of $\sim 73\%$ ([Ade et al. 2013c](#)), for the Planck map.

In order to assess the significance of any anisotropic signal in the data, we resort to simulated isotropic CMB maps. For the WMAP case, we generate 1000 CMB-plus-noise Monte Carlo (MC) simulations based on the WMAP9 best-fit Λ CDM power spectrum ([Hinshaw et al. 2013](#)). Noise realizations are drawn as uncorrelated Gaussian realizations with a spatially varying RMS distribution given by the number of observations per pixel; the WMAP simulations do not contain lensing effects. For Planck we adopt the 1000 “Full Focal Plane” (FFP6) end-to-end simulations produced by the Planck collaboration based on the instrument performance and noise properties. The FFP6 CMB and noise maps have been propagated through the Planck pipelines with the same weighting as the data. These simulations also incorporate lensing effects and are treated identically to the data in all steps discussed below. The doppler boosting effects, which have been shown to be an issue on small angular scales (high multipoles) ([Ade et al. 2013a](#)), have not been taken into account in this analysis. However, since variance is more sensitive to large angular scales

⁹ The look-elsewhere effect is a statistical effect that impacts the calculated significance of observing a local excess of events when searching for a signal in a possible range of a particular quantity without knowing a priori where the signal will appear within the range. This is especially severe if the significance is moderate. The significance calculation must account for the fact that an excess anywhere in the range could equally be considered as a signal. Therefore the look-elsewhere effect must be taken care of by taking into account the probability of observing a similar excess anywhere in the range (see e.g. [Gross and Vitells 2010](#)).

¹⁰ This refers to the cases where an anomalous feature is not predicted by any models before observing the data and is picked arbitrarily only after looking at the data. In other words, the feature is observed because the employed statistical method is designed to detect it.

(low multipoles), our results should not be significantly affected by these effects. We leave a full investigation of the Doppler boosting effects for future work.

The analysis proceeds as follows: We consider 3072 disks (of various sizes) centered on the pixels of a HEALPix $N_{\text{side}} = 16$ map¹¹ ([Górski et al. 2005](#)). For each disk and sky map, we compute the temperature variance including only unmasked pixels; any disk for which more than 90% of the area is masked is ignored completely. This results in a low-resolution and almost full-sky map of the local variance across the sky. To establish the expected mean and variance of each disk, we compute the same local-variance map from the simulated ensemble. This mean map is then subtracted from both the observed and simulated local-variance maps, resulting in a zero-mean variance variation map. Finally, we fit a dipole to each of these local-variance maps using the HEALPix `remove_dipole` routine using inverse variance weighting. Note that this procedure is strongly related to the Crossing statistic described by [Shafieloo et al. \(2011\)](#); [Shafieloo \(2012a,b\)](#), which has been applied to isotropy tests with low-redshift supernovae data ([Colin et al. 2011](#)).

3. ANALYSIS OF ANISOTROPIC SIMULATIONS

Before we discuss our results for the real data, we assess the sensitivity of the method by applying it to both simulated isotropic and anisotropic CMB realizations. The anisotropic simulations have been modulated by a dipole (Equation 1) with an amplitude of $A = 0.072$ and a direction of $(l, b) = (224^\circ, -22^\circ)$, consistent with that reported for large angular scales (e.g., [Hoftuft et al. 2009](#)). Two different sets of anisotropic simulations are generated, one for which all scales are modulated, and another for which only scales larger than 5° (corresponding to a 5° smoothing) have been modulated.

Figure 1 shows the resulting local-variance dipole amplitudes (top panel) and directions (bottom panels) as a function of disk radius for each of the 1000 FFP6 simulations, ranging between 1° and 90° .¹² Here we see that the sensitivity of the statistic depends significantly on the disk radius over which the variance is computed, and at a radius of $\sim 20^\circ$ even the amplitude distribution for the fully modulated model starts to overlap with the isotropic distribution. This makes intuitive sense, since the larger the radius, the more weight is put on the larger angular scales, and hence cosmic variance begins to dominate. For example, a radius of 20° corresponds roughly to angular features of $\ell \approx 180^\circ/20^\circ \approx 10$. This correspondence applies independently of the specific details of the assumed anisotropic model, and in the following we therefore restrict our interest to the range between 1° and 20° .

4. RESULTS

We now apply our variance estimator to the real WMAP and Planck data. First, Figure 2 shows the results for Planck, plotted in the same format as in Figure

¹¹ The results are not sensitive to the number of disks, as long as the entire sky is covered, and consistent results are obtained with, say, an $N_{\text{side}} = 8$ grid.

¹² The directions are shown only for anisotropic simulations; the resulting directions for isotropic simulations are uniformly distributed all over the sky and we do not show them here for brevity.

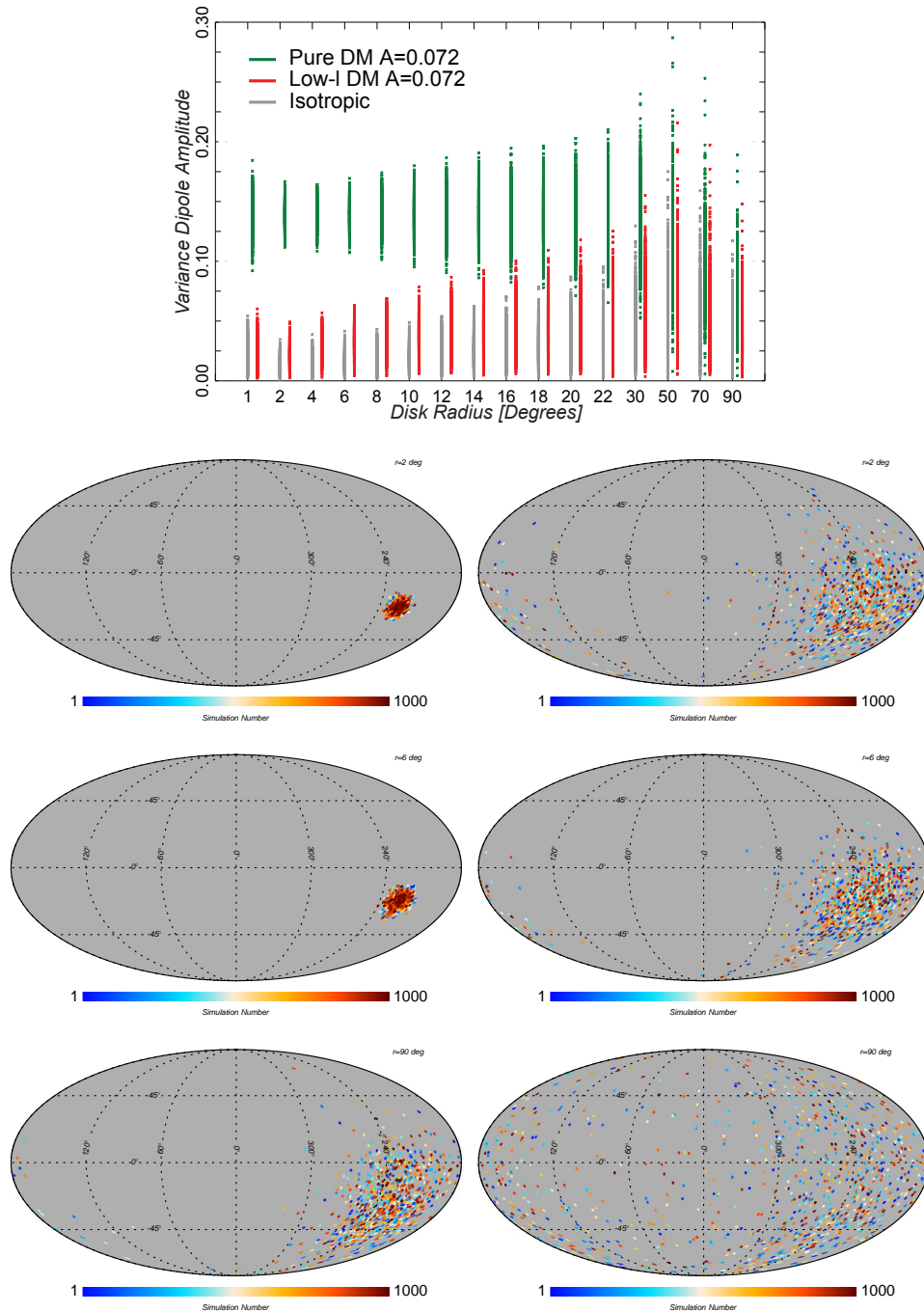


FIG. 1.— Upper panel: local-variance dipole amplitude as a function of disk radius for 1000 Planck (SMICA) FFP6 isotropic simulations (gray points), as well as for 1000 all-scale dipolar-modulated (pure DM; green points) and low-multipole-only (scales larger than 5°) dipolar-modulated (low- l DM; red points) simulations. Bottom panel: dipole directions recovered from all-scale (first column) and low-multipole-only (second column) dipolar-modulated simulations with disks of radii 2° , 6° and 90° . For all cases the input dipole amplitude and directions are $A = 0.072$ and $(l, b) = (224^\circ, -22^\circ)$.

1, but now comparing with the 1000 FFP6 isotropic simulations. As seen in the plot, none of the 1000 isotropic simulations have local-variance dipole amplitudes larger than the data over the range $6^\circ \leq r_{disk} \leq 12^\circ$, formally corresponding to a lower limit on the statistical significance of 3.3σ or a p -value of 0.001. To give a rough estimate of an actual significance, and not only a lower limit, we plot in Figure 3 histograms of the variance dipole amplitudes for the FFP6 simulations at the disk

radii with the highest detection significances, and fit a Gaussian in each case. Employing these extrapolations, we derive significances of $\sim 4\sigma$ in each of these cases. However, we emphasize that these numbers only serve as a rough guide, as the distributions do have significant non-Gaussian tails; an extended ensemble of simulations is certainly preferable over this approximation.

In order to see how a typical local-variance map, for a high-significance detection of asymmetry, looks like, we

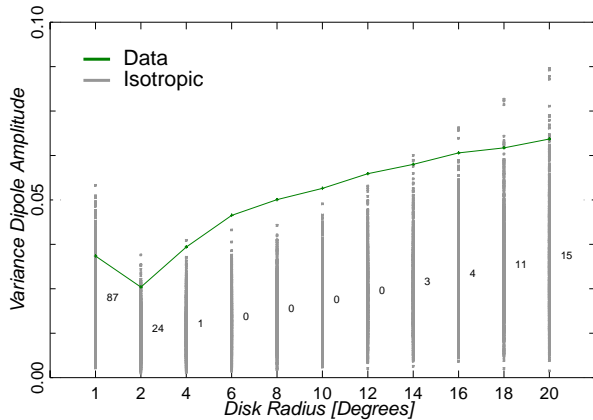


FIG. 2.— Local-variance dipole amplitude as a function of disk radius for Planck (SMICA) data (in green) versus the 1000 isotropic FFP6 simulations (in gray). The labels above each scale indicate the number of simulations with amplitudes larger than the ones estimated from the data, and are located at the means of the amplitude values from the simulations.

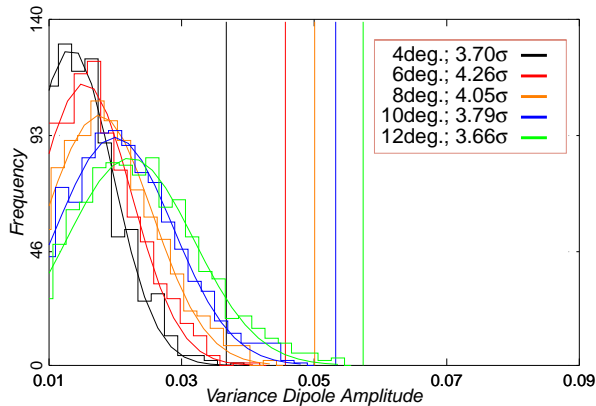


FIG. 3.— Histograms of the local-variance dipole amplitudes from the 1000 FFP6 simulations for disk radii 4° , 6° , 8° , 10° and 12° , together with the best-fit Gaussian distributions in all cases. Vertical lines indicate the corresponding amplitudes measured from the Planck data. The legend shows the rough estimates of detection significances derived from the Gaussian fits.

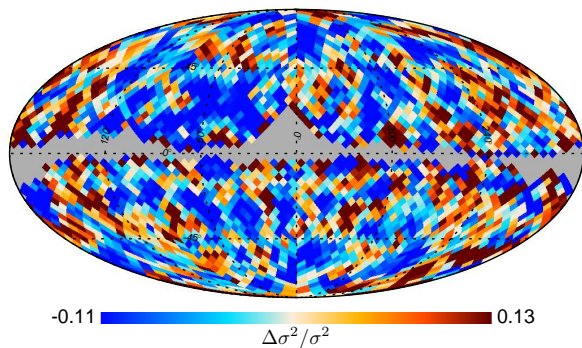


FIG. 4.— Mean-field subtracted, local-variance map computed with 6° disks for Planck (SMICA) data.

show in Figure 4 the mean-field subtracted map for 6° disks. Figure 5 shows the angular power spectrum of

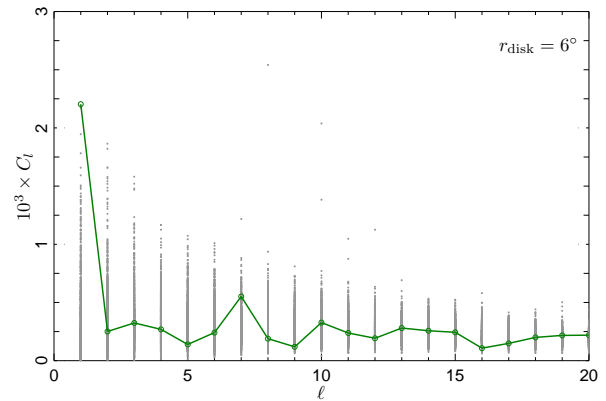


FIG. 5.— Angular power spectrum (C_ℓ) of the local-variance map computed with 6° disks for the 1000 FFP6 simulations (in gray), as well as for Planck (SMICA) data (in green).

TABLE 1
ASYMMETRY DIRECTIONS

Map	(l, b) [$^\circ$]	Significance or p -value	Reference
Planck-VA ^a	(212, -13)	0/1000	present work
WMAP9-VA	(219, -24)	5/1000	present work
Planck-DM	(227, -15)	3.5σ	<i>Ade et al. (2013a)</i>
WMAP5-DM	(224, -22)	3.3σ	<i>Hoftuft et al. (2009)</i>
Planck-PA	(218, -21)	0/500	<i>Ade et al. (2013a)</i>
WMAP9-PA	(227, -27)	7/10000	<i>Axelsson et al. (2013)</i>

^aVA, DM and PA stand for variance asymmetry, dipole modulation and power asymmetry, respectively.

the same map as a function of multipoles. This clearly shows that the dipole component is the dominant mode in the local-variance map. Figure 5 also indicates that the data is very consistent with isotropic simulations at all multipoles except for the dipole, which is anomalously large.

Similar results derived from the WMAP9 observations show qualitatively the same trend, but differ somewhat in terms of final significances (see Table 2). Specifically, a maximum asymmetry is seen between 6° and 12° , with ~ 5 out of 1000 isotropic simulations exhibiting a larger variance dipole amplitude, for a p -value of ~ 0.005 and a statistical significance of $\sim 2.9\sigma$.

The preferred directions obtained in the present paper (for 8° disks) are listed in Table 1, together with a number of similar results obtained in previous papers, and summarized visually in Figure 6. Clearly, the preferred directions derived by very different algorithms and data combinations are all in good qualitative agreement.

Ecliptic variance asymmetry:— Before we end this section, we present the results of a different, but related study, using variance as the statistic, which we have performed in addition to the main analysis of this paper. In *Ade et al. (2013a)* it is reported that the variances of the CMB fluctuations computed on the northern ecliptic and Galactic hemispheres are significantly smaller compared

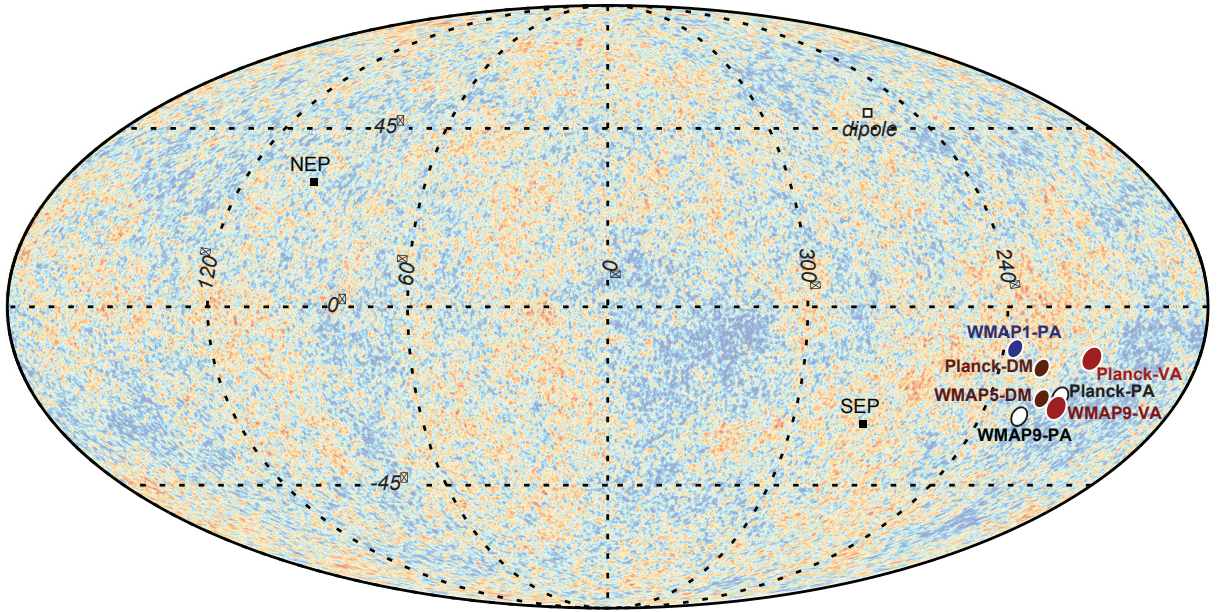


FIG. 6.— Asymmetry directions found in this work by analyzing the local variance of the WMAP 9-year and Planck 2013 data [denoted by *WMAP9-VA* and *Planck-VA*], as well as the directions found previously from the latest likelihood analyses of the dipole modulation model [denoted by *WMAP5-DM* (Hoftuft *et al.* 2009) and *Planck-DM* (Ade *et al.* 2013a)] and the local-power spectrum analyses [denoted by *WMAP1-PA* (Eriksen *et al.* 2004), *WMAP9-PA* (Axelsson *et al.* 2013) and *Planck-PA* (Ade *et al.* 2013a)] for the WMAP and Planck data. The background map is the CMB sky observed by Planck (SMICA). VA, DM and PA stand for variance asymmetry, dipole modulation and power asymmetry, respectively.

to the corresponding southern ones. We repeated the same analysis here, for the ecliptic hemispheres, and obtained similar results. A potential criticism of this study is the fact that it ignores look-elsewhere effects. This can be dealt with by using a test statistic, based on the differences in variances between different hemispheres, that involves a ranking procedure. Specifically, we first compute the difference in variances for each pair of opposite hemispheres for the data. By sorting the obtained values we assign a rank to for example the northern-southern ecliptic hemispheres. We then compare this value to the values with the same rank obtained from repeating the same procedure to all isotropic simulations, and derive a p -value. The p -value we obtain this way for the Planck data and FFP6 simulations shows that the variance difference along the ecliptic pole for the data is not significantly different from that of the isotropic simulations. However, performing the same procedure on the variance values for hemispheres (and not the variance differences) indicates that the variance from the northern ecliptic hemisphere for the data is still significantly low with a p -value of 4/1000.

5. SUMMARY

We have applied a simple local-variance estimator to the latest WMAP and Planck data, performing a frequentist test of global statistical isotropy. For the Planck data, we find that the local variance exhibits dipolar-like spatial variations that are statistically significant (at least) at the $\sim 3 - 3.5\sigma$ level on scales between $\sim 4^\circ$ and 14° by this measurement. For WMAP, we find a statistical significance of $\sim 2.9\sigma$, and a direction fully consistent with that derived from Planck.

The results obtained here are in good qualitative agreement with earlier results, for example using di-

rect likelihood fits or bipolar harmonics (Hoftuft *et al.* 2009; Ade *et al.* 2013a), that indicate a $\gtrsim 3\sigma$ dipole-modulation-like effect on large angular scales, but with an amplitude that is decreasing with angular scale. In the present approach, this is seen by the fact that the statistical significance decreases for the smallest disk radii of $1^\circ - 2^\circ$ scales; for a pure dipole modulation extending through all multipoles this stays constant.

The slight difference between Planck and WMAP can be mainly explained by the different masks that have been used in the two cases. In order to study the effects of the masks on the results, we repeated the analysis for both the WMAP and Planck maps using a unified mask, i.e. the combination of the Planck U73 and WMAP9 KQ85 masks. We obtained very similar results in these cases (see Table 2). The remaining differences can be at least partially explained by the different noise levels of the two experiments. No smoothing is applied to either data set in this analysis, and the variance therefore receives a significant contribution from the pixel-scale noise, which is substantially larger for WMAP than for Planck, decreasing the effective sensitivity of the estimator.

One should note however that choosing the right theoretical angular power spectrum for the isotropic simulations of the CMB maps is crucial and can also impact the obtained statistical significances, and might therefore provide another explanation for the differences in the significances computed from WMAP and Planck. It is known that (Ade *et al.* 2013d) there is a 1–2% mismatch between the power spectra computed from the two data sets and this can potentially explain some of the discrepancy that we see here. We have tested this effect by using the Planck best-fit power spectrum (Ade *et al.* 2013d) to

TABLE 2
COMPUTED VARIANCE ASYMMETRY SIGNIFICANCES WITH DIFFERENT DISK RADII

Data	Mask	C_ℓ used in simulations	2°	4°	6°	8°	10°	12°	14°	16°	18°	20°
WMAP9	KQ85	WMAP9 best-fit	101	28	7	5	6	6	9	15	20	27
Planck (SMICA)	U73	Planck best-fit	24	1	0	0	0	0	3	4	11	15
WMAP9	KQ85 + U73	WMAP9 best-fit	23	3	1	1	3	5	9	13	18	30
Planck (SMICA)	KQ85 + U73	Planck best-fit	16	1	1	0	1	3	7	9	13	22
WMAP9	KQ85	Planck best-fit	98	17	1	0	0	0	0	0	0	0

generate the simulations for WMAP. We observe that enforcing the Planck spectrum on the WMAP data makes the WMAP results comparable with the Planck ones. The significances for WMAP are now 0/1000 over disk radii of 8° – 22° (see Table 2), while the dipole directions do not change. This suggests, and remains to be investigated, that after resolving the tension between the Planck and WMAP power spectra the results of our analysis for the two experiments will agree better.

In this paper we have focussed on dipolar variations in the local-variance map, but this is clearly easily generalizable to higher-order modes. This will be considered in future work. For now, we note that the main advantages of the method are its conceptual and implementational simplicity, its directly intuitive interpretation, and, by virtue of being defined in pixel space, a useful complementarity to other typically harmonic-based methods. The fact that different statistical techniques, with different properties and sensitivities, result in very

similar conclusions does weaken the suggestion that the effect is simply the product of a-posteriori statistics.

We thank Claudio Llinares, Eamon M. Scullion and Amir Hajian for helpful discussions. Y.A. and H.K.E. acknowledge support through the ERC Starting Grant StG2010-257080. Y.F. is supported by ERC Grant 277742 Pascal. A.S. thanks the Korean Ministry of Education, Science and Technology (MEST), Gyeongsangbuk-Do and Pohang City for the support of the Independent Junior Research Groups at the Asia Pacific Center for Theoretical Physics (APCTP). F.K.H. acknowledges OYI grant from the Norwegian research council. We acknowledge the use of resources from the Norwegian national super-computing facilities, NOTUR. Maps and results have been derived using the HEALPix (<http://healpix.jpl.nasa.gov>) software package developed by Górski *et al.* (2005).

REFERENCES

- C. L. Bennett, M. Halpern, G. Hinshaw, N. Jarosik, A. Kogut, M. Limon, S. S. Meyer, L. Page, D. N. Spergel, G. S. Tucker, E. Wollack, E. L. Wright, C. Barnes, M. R. Greason, R. S. Hill, E. Komatsu, M. R. Nolte, N. Odegard, H. V. Peiris, L. Verde, and J. L. Weiland, *ApJS* **148**, 1 (2003), [arXiv:astro-ph/0302207](https://arxiv.org/abs/astro-ph/0302207).
- M. Tegmark, A. de Oliveira-Costa, and A. Hamilton, *Phys.Rev.* **D68**, 123523 (2003), [arXiv:astro-ph/0302496](https://arxiv.org/abs/astro-ph/0302496) [astro-ph].
- A. de Oliveira-Costa, M. Tegmark, M. Zaldarriaga, and A. Hamilton, *Phys.Rev.* **D69**, 063516 (2004), [arXiv:astro-ph/0307282](https://arxiv.org/abs/astro-ph/0307282) [astro-ph].
- P. Vielva, E. Martinez-Gonzalez, R. Barreiro, J. Sanz, and L. Cayon, *Astrophys.J.* **609**, 22 (2004), [arXiv:astro-ph/0310273](https://arxiv.org/abs/astro-ph/0310273) [astro-ph].
- D. L. Larson and B. D. Wandelt, *Astrophys.J.* **613**, L85 (2004), [arXiv:astro-ph/0404037](https://arxiv.org/abs/astro-ph/0404037) [astro-ph].
- K. Land and J. Magueijo, *Mon.Not.Roy.Astron.Soc.* **357**, 994 (2005a), [arXiv:astro-ph/0405519](https://arxiv.org/abs/astro-ph/0405519) [astro-ph].
- K. Land and J. Magueijo, *Phys.Rev.Lett.* **95**, 071301 (2005b), [arXiv:astro-ph/0502237](https://arxiv.org/abs/astro-ph/0502237) [astro-ph].
- J. D. McEwen, M. Hobson, A. Lasenby, and D. Mortlock, *Mon.Not.Roy.Astron.Soc.* **359**, 1583 (2005), [arXiv:astro-ph/0406604](https://arxiv.org/abs/astro-ph/0406604) [astro-ph].
- J. D. McEwen, M. Hobson, A. Lasenby, and D. Mortlock, *Mon.Not.Roy.Astron.Soc.* **371**, L50 (2006), [arXiv:astro-ph/0604305](https://arxiv.org/abs/astro-ph/0604305) [astro-ph].
- T. Jaffe, A. Banday, H. Eriksen, K. Gorski, and F. Hansen, *Astron.Astrophys.* **460**, 393 (2006), [arXiv:astro-ph/0606046](https://arxiv.org/abs/astro-ph/0606046) [astro-ph].
- G. Hinshaw *et al.* (WMAP Collaboration), *Astrophys.J.Suppl.* **170**, 288 (2007), [arXiv:astro-ph/0603451](https://arxiv.org/abs/astro-ph/0603451) [astro-ph].
- D. Spergel *et al.* (WMAP Collaboration), *Astrophys.J.Suppl.* **170**, 377 (2007), [arXiv:astro-ph/0603449](https://arxiv.org/abs/astro-ph/0603449) [astro-ph].
- M. Cruz, L. Cayon, E. Martinez-Gonzalez, P. Vielva, and J. Jin, *Astrophys.J.* **655**, 11 (2007), [arXiv:astro-ph/0603859](https://arxiv.org/abs/astro-ph/0603859) [astro-ph].
- M. Bridges, J. McEwen, A. Lasenby, and M. Hobson, *Mon.Not.Roy.Astron.Soc.* **377**, 1473 (2007), [arXiv:astro-ph/0605325](https://arxiv.org/abs/astro-ph/0605325) [astro-ph].
- C. Copi, D. Huterer, D. Schwarz, and G. Starkman, *Phys.Rev.* **D75**, 023507 (2007), [arXiv:astro-ph/0605135](https://arxiv.org/abs/astro-ph/0605135) [astro-ph].
- K. Land and J. Magueijo, *Mon.Not.Roy.Astron.Soc.* **378**, 153 (2007), [arXiv:astro-ph/0611518](https://arxiv.org/abs/astro-ph/0611518) [astro-ph].
- A. Bernui, B. Mota, M. J. Rebouças, and R. Tavakol, *Astron.Astrophys.* **464**, 479 (2007), [arXiv:astro-ph/0511666](https://arxiv.org/abs/astro-ph/0511666) [astro-ph].
- A. Bernui and W. Hipolito-Ricardi, *Mon.Not.Roy.Astron.Soc.* **389**, 1453 (2008), [arXiv:0807.1076](https://arxiv.org/abs/astro-ph/0807.1076) [astro-ph].
- D. Pietrobon, A. Amblard, A. Balbi, P. Cabella, A. Cooray, *et al.*, *Phys.Rev.* **D78**, 103504 (2008), [arXiv:0809.0010](https://arxiv.org/abs/astro-ph/0809.0010) [astro-ph].
- H. K. Eriksen, F. K. Hansen, A. J. Banday, K. M. Gorski, and P. B. Lilje, *ApJ* **605**, 14 (2004), [arXiv:astro-ph/0307507](https://arxiv.org/abs/astro-ph/0307507).
- F. K. Hansen, A. J. Banday, and K. M. Górski, *MNRAS* **354**, 641 (2004), [arXiv:astro-ph/0404206](https://arxiv.org/abs/astro-ph/0404206).
- C. G. Park, *MNRAS* **349**, 313 (2004), [arXiv:astro-ph/0307469](https://arxiv.org/abs/astro-ph/0307469) [astro-ph.CO].
- H. K. Eriksen, A. Banday, K. Gorski, F. Hansen, and P. Lilje, *Astrophys.J.* **660**, L81 (2007), [arXiv:astro-ph/0701089](https://arxiv.org/abs/astro-ph/0701089) [astro-ph].
- F. K. Hansen, A. J. Banday, K. M. Gorski, H. K. Eriksen, and P. B. Lilje, *ApJ* **704**, 1448 (2009), [arXiv:0812.3795](https://arxiv.org/abs/astro-ph/0812.3795) [astro-ph].

- J. Hoftuft, H. K. Eriksen, A. J. Banday, K. M. Gorski, F. K. Hansen, and P. B. Lilje, *ApJ* **699**, 985 (2009), [arXiv:0903.1229 \[astro-ph.CO\]](#).
- M. Axelsson, Y. Fantaye, F. Hansen, A. Banday, H. Eriksen, *et al.*, *Astrophys.J.* **773**, L3 (2013), [arXiv:1303.5371 \[astro-ph.CO\]](#).
- P. Ade *et al.* (Planck Collaboration), (2013a), [arXiv:1303.5083 \[astro-ph.CO\]](#).
- A. L. Erickcek, M. Kamionkowski, and S. M. Carroll, *Phys.Rev.* **D78**, 123520 (2008), [arXiv:0806.0377 \[astro-ph\]](#).
- L. Dai, D. Jeong, M. Kamionkowski, and J. Chluba, *Phys.Rev.* **D87**, 123005 (2013), [arXiv:1303.6949 \[astro-ph.CO\]](#).
- D. H. Lyth, *JCAP* **1308**, 007 (2013), [arXiv:1304.1270 \[astro-ph.CO\]](#).
- A. R. Liddle and M. Corts, (2013), 10.1103/PhysRevLett.111.111302, [arXiv:1306.5698 \[astro-ph.CO\]](#).
- A. Mazumdar and L. Wang, (2013), [arXiv:1306.5736 \[astro-ph.CO\]](#).
- M. H. Namjoo, S. Baghram, and H. Firouzjahi, *Phys.Rev.* **D88**, 083527 (2013), [arXiv:1305.0813 \[astro-ph.CO\]](#).
- A. A. Abolhasani, S. Baghram, H. Firouzjahi, and M. H. Namjoo, (2013), [arXiv:1306.6932 \[astro-ph.CO\]](#).
- Y.-F. Cai, W. Zhao, and Y. Zhang, (2013), [arXiv:1307.4090 \[astro-ph.CO\]](#).
- K. Kohri, C.-M. Lin, and T. Matsuda, (2013), [arXiv:1308.5790 \[hep-ph\]](#).
- J. McDonald, (2013), [arXiv:1309.1122 \[astro-ph.CO\]](#).
- S. Kanno, M. Sasaki, and T. Tanaka, (2013), [arXiv:1309.1350 \[astro-ph.CO\]](#).
- C. Gordon, W. Hu, D. Huterer, and T. Crawford, *Phys. Rev. D* **72**, 103002 (2005), [arXiv:astro-ph/0509301](#).
- P. Ade *et al.* (Planck Collaboration), (2013b), [arXiv:1303.5062 \[astro-ph.CO\]](#).
- A. Hajian and T. Souradeep, *Astrophys.J.* **597**, L5 (2003), [arXiv:astro-ph/0308001 \[astro-ph\]](#).
- A. Hajian and T. Souradeep, *Phys.Rev.* **D74**, 123521 (2006), [arXiv:astro-ph/0607153 \[astro-ph\]](#).
- E. Gross and O. Vitells, *European Physical Journal C* **70**, 525 (2010), [arXiv:1005.1891 \[physics.data-an\]](#).
- C. L. Bennett, R. S. Hill, G. Hinshaw, D. Larson, K. M. Smith, J. Dunkley, B. Gold, M. Halpern, N. Jarosik, A. Kogut, E. Komatsu, M. Limon, S. S. Meyer, M. R. Nolta, N. Odegard, L. Page, D. N. Spergel, G. S. Tucker, J. L. Weiland, E. Wollack, and E. L. Wright, *ApJS* **192**, 17 (2011), [arXiv:1001.4758 \[astro-ph.CO\]](#).
- B. Lew, *JCAP* **0809**, 023 (2008a), [arXiv:0808.2867 \[astro-ph\]](#).
- B. Lew, *JCAP* **0808**, 017 (2008b), [arXiv:0803.1409 \[astro-ph\]](#).
- P. K. Rath and P. Jain, (2013), [arXiv:1308.0924 \[astro-ph.CO\]](#).
- P. Ade *et al.* (Planck Collaboration), (2013c), [arXiv:1303.5072 \[astro-ph.CO\]](#).
- G. Hinshaw *et al.* (WMAP), *Astrophys.J.Suppl.* **208**, 19 (2013), [arXiv:1212.5226 \[astro-ph.CO\]](#).
- K. M. Górski, E. Hivon, A. J. Banday, B. D. Wandelt, F. K. Hansen, M. Reinecke, and M. Bartelmann, *ApJ* **699**, 759 (2005), [arXiv:astro-ph/0409513](#).
- A. Shafieloo, T. Clifton, and P. G. Ferreira, *JCAP* **1108**, 017 (2011), [arXiv:1006.2141 \[astro-ph.CO\]](#).
- A. Shafieloo, *JCAP* **1205**, 024 (2012a), [arXiv:1202.4808 \[astro-ph.CO\]](#).
- A. Shafieloo, *JCAP* **1208**, 002 (2012b), [arXiv:1204.1109 \[astro-ph.CO\]](#).
- J. Colin, R. Mohayaee, S. Sarkar, and A. Shafieloo, *Mon.Not.Roy.Astron.Soc.* **414**, 264 (2011), [arXiv:1011.6292 \[astro-ph.CO\]](#).
- P. Ade *et al.* (Planck collaboration), (2013d), [arXiv:1303.5075 \[astro-ph.CO\]](#).